

## Robust test of E(5) symmetry in $^{128}\text{Xe}$

L. Coquard,<sup>1</sup> N. Pietralla,<sup>1</sup> T. Ahn,<sup>1,2</sup> G. Rainovski,<sup>3</sup> L. Bettermann,<sup>4</sup> M. P. Carpenter,<sup>5</sup> R. V. F. Janssens,<sup>5</sup> J. Leske,<sup>1</sup> C. J. Lister,<sup>5</sup> O. Möller,<sup>1</sup> W. Rother,<sup>4</sup> V. Werner,<sup>2</sup> and S. Zhu<sup>5</sup>

<sup>1</sup>*Institut für Kernphysik, Technische Universität Darmstadt, D-64289 Darmstadt, Germany*

<sup>2</sup>*Wright Nuclear Structure Laboratory, Yale University, New Haven, Connecticut 06520, USA*

<sup>3</sup>*Faculty of Physics, St. Kliment Ohridski University of Sofia, 1164 Sofia, Bulgaria*

<sup>4</sup>*Institut für Kernphysik, Universität Köln, Zùlpicher Str. 77, D-50937 Köln, Germany*

<sup>5</sup>*Physics Division, Argonne National Laboratory, Argonne, IL 60439, USA*

(Received 16 November 2009; published 23 December 2009)

Low-lying collectively excited states of  $^{128}\text{Xe}$  were investigated by  $\gamma$ -ray spectroscopy following the  $^{12}\text{C}(^{128}\text{Xe}, ^{128}\text{Xe}^*)^{12}\text{C}$  projectile Coulomb excitation reaction. Nineteen absolute  $E2$  transition strengths were obtained including the first measurement of the critical  $B(E2)$  decays from the second and third  $J^\pi = 0^+$  states. These data are compared with the theoretical predictions of the critical point symmetry E(5) and allow us to conclude that  $^{128}\text{Xe}$  is not an E(5) nucleus as previously suggested, leaving  $^{130}\text{Xe}$  as the most likely candidate among the Xe isotopes.

DOI: [10.1103/PhysRevC.80.061304](https://doi.org/10.1103/PhysRevC.80.061304)

PACS number(s): 21.10.Re, 23.20.Js, 25.70.De, 27.60.+j

The solutions of the Bohr Hamiltonian for a variety of geometric potentials by Iachello and collaborators [1–3] has provided considerable new intuitive insight into shape transitions. One transition, the E(5) symmetry [1], reflects the critical point in the shape transition from spherical to  $\gamma$ -soft, O(6)-like nuclei. The shape transitional point and also the E(5) symmetry are characterized by large fluctuations in the quadrupole deformation parameter  $\beta$  and maximum fluctuations in the triaxiality parameter  $\gamma$ . This leads to characteristic ratios between excitation energies of various excited states and between their  $E2$  transition rates. As Xe and Ba are thought to be  $\gamma$ -soft, candidates for E(5) symmetry should be expected in this region as the spherical  $N = 82$  shell closure is approached. Casten and Zamfir [4] suggested  $^{134}\text{Ba}$  as a possible realization of the E(5) tipping point, based on a few simple experimental signatures such as the  $R_{4/2} = E(4_1^+)/E(2_1^+)$  ratio and the relative excitation energies  $R_{0/2} = E(0_{2,3}^+)/E(2_1^+)$  and  $E2$  decay branching ratios of the first two excited  $0^+$  states.

Subsequently, Clark and collaborators [5] conducted a systematic search of the nuclear databases for the occurrence of experimental fingerprints of E(5) symmetry.  $R_{4/2}$  and  $R_{0/2}$  ratios pointed at the nucleus  $^{128}\text{Xe}$  as another possible realization of E(5) symmetry [5]. This conclusion implies that  $^{128}\text{Xe}$  is near the shape-phase transition from spherical nuclei around the doubly closed-shell nucleus  $^{132}\text{Sn}$  to the deformed  $\gamma$ -soft nuclei for which the  $A \approx 130$  mass region is well known [6]. In fact, this mass region is considered the largest region of the nuclear chart with  $\gamma$ -soft nuclei. However, the loci of phase transitional lines between spherical and  $\gamma$ -softly deformed nuclei are not yet established in this mass region.

Recently, Bonatsos and collaborators formulated the  $\gamma$ -independent version [7] of the confined beta-soft (CBS) rotor model [8]. That version, called O(5)-CBS, generalizes the E(5) solution near the critical point to a parametric solution for the whole path between E(5) and the  $\beta$ -rigidly deformed  $\gamma$ -independent limit. The structure of  $^{128}\text{Xe}$  was investigated in terms of the O(5)-CBS [7]. The decay pattern of the

first two excited  $0^+$  states suggest that  $^{128}\text{Xe}$  is already located well beyond the U(5)-O(6) shape-phase transition in the deformed phase. The previous suggestion by Clark and collaborators for the critical structure of  $^{128}\text{Xe}$  was mainly based on relative excitation energies, absolute  $B(E2)$  strengths in the ground-state band as well as for the  $2_2^+$  state, and the branching ratio of the  $0_2^+$  state and one known branch from the  $0_3^+$  state ( $0_3^+$  to  $2_1^+$ ). In Ref. [5], the  $0_2^+$  and  $0_3^+$  states were assigned as  $0_\tau^+$  and  $0_\xi^+$ , respectively. Bonatsos and collaborators investigated the  $E2$  decay branching ratio of the  $0_3^+$  state and found supporting evidence for these assignments. However, the arguments of Bonatsos and collaborators relied on the analysis of  $E2$   $\gamma$ -ray branching ratios of which at least one had a large experimental uncertainty ( $\sim 50\%$ ). The  $E2$  branching ratios further suggested that the crucial excited  $0^+$  states were mixed in a two-state mixing scheme. That scheme led to a satisfactory description of excitation energies and branching ratios, but its consistency with data cannot be tested independently without the knowledge of absolute  $B(E2)$  values. Due to the importance of the  $A \approx 130$  mass region for the issue of a possible U(5)-O(6) phase transitional point, it is highly desirable to improve on the uncertainty for the  $E2$  decay branching ratios of excited  $0^+$  states of  $^{128}\text{Xe}$  and even more to gain information on the corresponding absolute  $B(E2)$  values for a quantitative test of the arguments made by Bonatsos and collaborators [7]. The purpose of this rapid communication is to report on the results of the measurement of absolute  $E2$  decay strengths from both lowest-lying excited  $0^+$  states ( $0_2^+$  and  $0_3^+$ ) of  $^{128}\text{Xe}$  in order to check quantitatively on the two-state mixing scheme and the structure assignments for the  $0^+$  states of  $^{128}\text{Xe}$ . This rapid communication settles the question of whether  $^{128}\text{Xe}$  is a strong candidate for a realization of E(5) symmetry.

The experiment was performed at Argonne National Laboratory. The superconducting ATLAS accelerator provided a beam of  $^{128}\text{Xe}$  ions with an energy of 404 MeV. This energy corresponds to  $\sim 82\%$  of the Coulomb barrier for the reaction of  $^{128}\text{Xe}$  on a  $^{12}\text{C}$  target. The beam intensity was

$\sim 1$  pnA. The beam was pulsed (12 MHz) and impinged on a natural  $^{12}\text{C}$  target of  $1\text{ mg/cm}^2$ . The emitted  $\gamma$ -rays were detected by the Gammasphere array, which consisted of 98 high-purity Compton suppressed germanium detectors arranged in 16 rings [9,10]. An event trigger was defined by the detection of at least one unsuppressed  $\gamma$ -ray of multiplicity 1 or higher. The Gammasphere was operated in pure “singles” mode with an average trigger readout rate of 15,000 events/s with multiplicity  $> 1$ . The readout dead time was  $\sim 30\%$ . This count rate compares with the “beam-off” rate of 600 triggers/s. Doppler correction [recoiling velocity  $\beta = 6.5(2)\%$ ] and time-random background subtraction was applied. As the beam energy was relatively low, the dominant “beam-off” count rate came from natural sources. This background was identified and subtracted by selecting events from between the beam bursts and scaled to eliminate the 1461 keV decay from  $^{40}\text{K}$ . The singles spectrum is displayed in Fig. 1. The total number of events was  $1.0 \times 10^9$  for a running time of  $\sim 23$  h. Approximately  $1.7 \times 10^7$  events of the  $\gamma$ -ray fold higher than one were collected and sorted into a  $\gamma\gamma$  coincidence matrix. All the  $\gamma$ -transitions observed were placed in the level scheme of  $^{128}\text{Xe}$  (Fig. 2). Their corresponding intensities are listed in Table I. Information on these levels was reported previously in Refs. [11–15]. The  $\gamma$ -ray intensities were normalized to the  $2_1^+ \rightarrow 0_1^+$  transition, which dominates the spectrum by three orders of magnitude. Population yields of each state were deduced from  $\gamma$ -singles and  $\gamma\gamma$ -coincidence data. The contributions from the electron conversion decays to the populations of the states were small in comparison to the systematic errors ( $< 1.5\%$ , [16]) and were neglected. The contributions of known transitions that we were not able to observe (e.g., due to too small energy or contaminations) were determined from the previously published branching ratios from Ref. [17].

The observed relative yields measure the Coulomb excitation (CE) cross sections relative to the  $2_1^+$  state. The code CLX, based on the Winther-De Boer theory [18], was used to determine the matrix elements for reproducing the observed relative cross sections.

The previously known  $B(E2; 2_1^+ \rightarrow 0_1^+) = 0.165(25)e^2b^2$  value from Ref. [19] sets the absolute scale. The energy loss of the beam inside the target ( $\sim 40$  MeV) was taken into account. The unknown quadrupole moments of excited states were allowed to vary between the extreme rotational

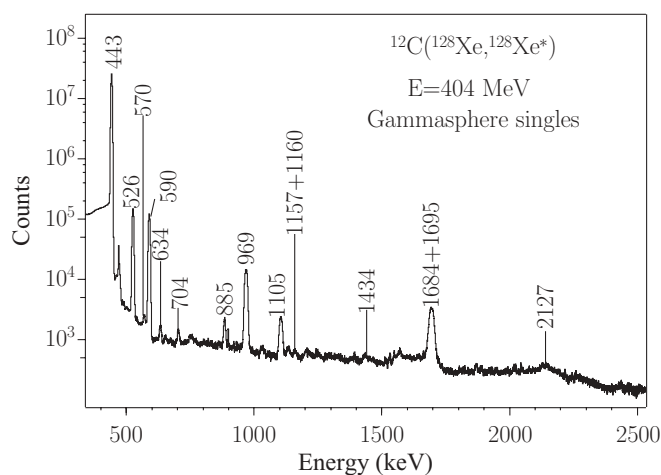


FIG. 1. Doppler-corrected and background-subtracted  $\gamma$ -ray spectrum for the sum of all detectors in Gammasphere.

limits ( $Q = \pm 2.74 eb$ ) adding uncertainties to the transitional matrix elements of about 3% on average. The input matrix elements in CLX were also constrained by the known branching and multipole mixing ratios. The resulting  $B(E2)$  transition strengths are given in Table I. The choice of signs of the matrix elements is not always unique in a fit to multistep Coulomb excitation processes. However, constraints come from the requirement that the relative phases must be “quantum mechanically coherent” as outlined by Wu and collaborators [20]. The chosen signs ( $\sigma$ ) of the  $E2$  matrix elements are included in Table I. Our analysis resulted in 19 absolute and 7 upper limits for  $B(E2)$  values. This comprehensive data set can be used for a robust test of the previously debated [5,7] possible E(5) character of  $^{128}\text{Xe}$ . We note that our results are in very good agreement with the previously known  $B(E2)$  [17], as well as the  $B(E3)\uparrow$  [19], which verifies our analysis procedure. To test the E(5) character of  $^{128}\text{Xe}$  quantitatively, we focus on sensitive key observables that are listed in Table II along with the corresponding predictions of relevant models. For further details concerning the different models, refer to Refs. [1,5,7]. An important signature for the E(5) critical point is the ratio  $R_{4/2}$ . In the case of  $^{128}\text{Xe}$ , this observable is  $R_{4/2} = 2.33$  intermediate between the value for E(5) ( $R_{4/2} = 2.20$ ) and the deformed  $\gamma$ -independent limit or O(6) ( $R_{4/2} = 2.50$ ). The

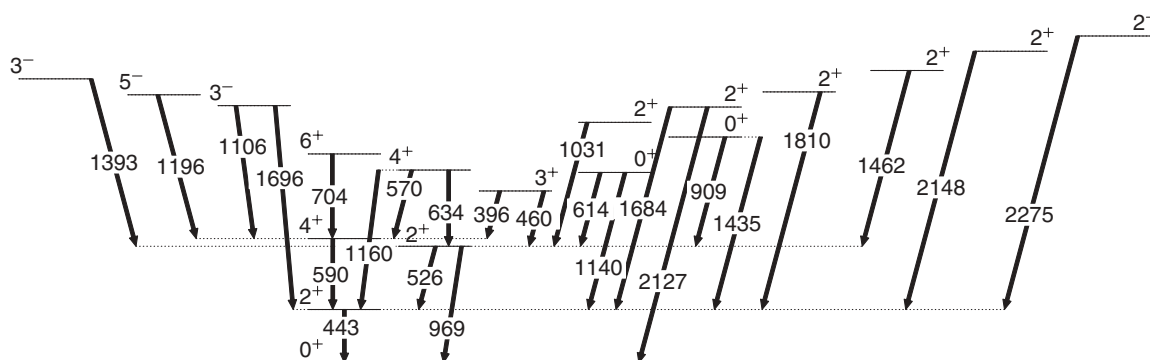


FIG. 2. A low-spin level scheme of  $^{128}\text{Xe}$  with the corresponding  $\gamma$ -ray transitions observed in our experiment.

TABLE I. Transition strengths of the low-lying Coulomb excited states of  $^{128}\text{Xe}$ .

$E_{\text{level}}$ (keV)	$J^\pi$	$E_\gamma$ (keV)	$I_\gamma$	$J_{\text{final}}^\pi$	$\delta^a$	$\sigma$	$B(E2)^b$ W.u.
442.9	$2_1^+$	442.9	$10^6$	$0_1^+$		+	42.6(64) <sup>c</sup>
969.5	$2_2^+$	526.5	7271(51)	$2_1^+$	+4.4(7)	−	50.1(97)
		969.5 <sup>d</sup>	1855(16)	$0_1^+$		+	0.65(8)
1033.1	$4_1^+$	590.2	7043(49)	$2_1^+$		+	63.5(52)
1429.6	$3_1^+$	396.3 <sup>e</sup>	1.73(27)	$4_1^+$	+2.8(3)	−	31.8(59)
		460.1 <sup>f</sup>	9.4(14)	$2_2^+$	+7.8(8)	+	91(16)
		986.6 <sup>e</sup>	8.9(14)	$2_1^+$	+1.7(1)	−	1.45(26)
1583.0	$0_2^+$	613.5 <sup>f</sup>	6.1(12)	$2_2^+$		+	52.8(76)
		1140.0 <sup>e</sup>	10.4(12)	$2_1^+$		−	3.69(58)
1603.5	$4_2^+$	570.4	36.2(8)	$4_1^+$	+1.9 <sub>0.5</sub> <sup>g</sup>	+	30.2(32)
		634.0	50.4(8)	$2_2^+$		−	29.6(29)
		1160.6 <sup>d</sup>	18.2(7)	$2_1^+$		−	0.52(6)
1737.3	$6_1^+$	704.2	40.7(14)	$4_1^+$		+	106(13)
1877.7	$0_3^+$	908.2 <sup>f</sup>	5.4(9)	$2_2^+$		+	22.2(46)
		1434.4	27.8(30)	$2_1^+$		−	10.4(23)
2127.1	$2_4^+$	1157.5 <sup>d</sup>	5.7(5)	$2_2^+$		+	$\leq 0.74(113)^g$
		1684.1 <sup>d</sup>	90(15)	$2_1^+$	+0.08(6)	+	0.035(54)
				$2_1^+$			$B(M1) = 0.042(12)\mu_N^2$
		2127.1	11.0(13)	$0_1^+$		+	0.21(7)
2138.7	$3_1^-$	1105.4	267(3)	$4_1^+$		+	
		1695.8 <sup>d</sup>	861(19)	$2_1^+$		+	
		2138.7		$0_1^+$		+	0.069(14) <sup>h</sup>
2165.9		1132.7 <sup>d</sup>	16.4(20)	$4_1^+$			
2229.2	$(5)_1^-$	1196.1 <sup>f</sup>	8.9(11)	$4_1^+$			
2361.6	(3)	1392.1 <sup>f</sup>	14.7(11)	$2_2^+$			
2430.7	$2^+$	1461.2 <sup>f</sup>	6.3(8)	$2_2^+$		−	$\leq 2.30(85)$
		1987.8 <sup>e</sup>	5.8(5)	$2_1^+$		−	$\leq 0.48(18)$
		2430.7 <sup>e</sup>	1.3(1)	$0_1^+$		+	0.15(6)
2591.6	$2^+$	1162.0 <sup>e</sup>	4.9(8)	$3_1^+$		+	$\leq 22.9(68)$
		2148.6 <sup>f</sup>	24.4(21)	$2_1^+$		+	$\leq 5.3(13)$
		2591.5 <sup>e</sup>	0.75(9)	$0_1^+$		+	0.98(27)
2718.5	$2^+$	1749.0 <sup>e</sup>	5.2(17)	$2_2^+$		+	$\leq 11.3(47)$
		2275.6 <sup>f</sup>	23.5(20)	$2_1^+$		+	$\leq 13.8(36)$
		2718.5 <sup>e</sup>	0.13(4)	$0_1^+$		+	1.23(51)

<sup>a</sup>Mixing ratios are taken from Ref. [17].

<sup>b</sup> $B(E2)$  values are given in W.u. (1 W.u.(E2) = 0.0038318  $e^2b^2$ ), and the  $B(E3; 0_1^+ \rightarrow 3_1^-)\uparrow$  value is given in  $e^2b^3$ .

<sup>c</sup>From Ref. [19].

<sup>d</sup>These transitions are doublets. Their respective intensities have been separated through the known branching ratios from Ref. [17].

<sup>e</sup>These transitions are not observed by us but are included in the calculations for the Coulomb cross-sections. Their intensities are deduced from the previously known branching ratios from Ref. [17].

<sup>f</sup>These transitions were seen only in our coincidence spectra.

<sup>g</sup>Upper value for the  $B(E2)$  since the mixing ratio was unknown, quoted value obtained by assuming a pure E2 transition.

<sup>h</sup>In Ref. [19], a  $B(E3)\uparrow = 0.083(11) e^2b^3$  value is reported.

$R_{4/2}$  ratio suggests that  $^{128}\text{Xe}$  should lie between E(5) and O(6).

Other key features of the E(5) critical-point symmetry are the properties of the  $0_2^+$  and  $0_3^+$  states that vary along the U(5)-O(6) transition. A major difference between these two limits, besides the relative energies of the multiplets, is the structure of the excited  $0^+$  states. One of them is a member of the three-phonon multiplet with O(5) quantum number [1,21]  $\tau = 3$  in the entire transition U(5)-O(6) (denoted  $0_\tau^+$ ). The other one (denoted  $0_\xi^+$ ) evolves from the two-phonon  $0^+$  state in U(5), with a strong  $B(E2; 0_{2\text{ph}}^+ \rightarrow 2_1^+)$  value, into the band-

head of the  $\sigma = N - 2$  family in O(6), where it typically lies higher than the  $0_\tau^+$  state and the  $B(E2; 0_{N-2}^+ \rightarrow 2_1^+)$  value vanishes. In fact, these  $0^+$  states test the softness of the nuclear potential in the deformation variables  $\beta$  and  $\gamma$ .

The evolution of these two  $0^+$  states between E(5) and the rigidly deformed  $\gamma$ -independent rotor limit [i.e., the O(6) symmetry of the infinite boson number (IBM)] is predicted by the O(5)-CBS rotor model [7]. In E(5) the  $0_\xi^+$  state lies below the  $0_\tau^+$  state. With increasing nuclear rigidity the excitation energies relative to the  $2_1^+$  state ( $R_{0/2}$ ) increase monotonically for both of them. The  $R_{0/2}$  value of the  $0_\xi^+$  state increases more

TABLE II. Comparison of key observables in  $^{128}\text{Xe}$ : For the experimental values taken from this work and Ref. [17] ( $^{128}\text{Xe}$ ), for the experimental values including a two-state mixing ( $^{128}\text{Xe}^*$ , see text), for the pure E(5) symmetry [1] [row denoted E(5)], and for the O(5)-confined  $\beta$ -soft rotor model [7] with the structural parameter  $r_\beta = 0.21$  [row denoted O(5)-CBS].

	$R_{4/2}$	$R_{0_2^+ / 2}$	$R_{0_3^+ / 2}$	$\frac{B(E2; 4_1^+ \rightarrow 2_1^+)}{B(E2; 2_1^+ \rightarrow 0_1^+)}$	$\frac{B(E2; 0_2^+ \rightarrow 2_2^+)}{B(E2; 2_1^+ \rightarrow 0_1^+)}$	$\frac{B(E2; 0_\xi^+ \rightarrow 2_1^+)}{B(E2; 2_1^+ \rightarrow 0_1^+)}$	$\frac{B(E2; 0_\xi^+ \rightarrow 2_1^+)}{B(E2; 0_\tau^+ \rightarrow 2_2^+)}$
$^{128}\text{Xe}$	2.33	3.57	4.24	1.49(25)	1.24(26)	0.24(6)	0.19(6)
$^{128}\text{Xe}^*$	2.33	3.76	4.05	1.49(25)	1.78(36)	0.33(7)	0.18(5)
E(5)	2.19	3.59	3.03	1.68	2.21	0.86	0.39
O(5)-CBS	2.32	3.88	4.27	1.57	2.00	0.52	0.26

strongly than that of the  $0_\tau^+$  state. Consequently, these levels cross as a function of the rigidity of the nuclear potential in the quadrupole deformation variable  $\beta$ . Eventually the  $R_{0/2}(0_\xi^+)$  becomes infinite toward the rigid limit [7].

Along this evolutionary path, the O(5) vibration-like symmetry is preserved and the  $\Delta\tau = 2$  E2 transitions,  $0_\tau^+ \rightarrow 2_1^+$  and  $0_\xi^+ \rightarrow 2_2^+$ , are forbidden in leading order due to the selection rule  $\Delta\tau = \pm 1$  for the E2 operator [1,7,21]. For the same reason, the  $0_\tau^+ \rightarrow 2_2^+$  and  $0_\xi^+ \rightarrow 2_1^+$  E2 transitions are allowed up to the rigid limit. This suggests a structure assignment to these  $0^+$  states already from their E2 decay branching pattern. In this respect, the relative position of the  $0_{\xi,\tau}^+$  states and their absolute  $B(E2)$  values are the most sensitive key features of E(5) symmetry (Table II). In  $^{128}\text{Xe}$  the situation is, however, more complicated and the unambiguous assignment needs to be based on the knowledge of absolute E2 decay rates from our new data. The  $0_2^+$  state at 1582.9 keV is assigned to be the  $0_\tau^+$  state. It decays strongly to the  $2_2^+$  state [ $B(E2; 0_2^+ \rightarrow 2_2^+) = 52.8(76)$  W.u.]. This behavior confirms the three-phonon-like nature of the  $0_2^+$  state. Note that there is also a weak decay to the  $2_1^+$  state [ $B(E2; 0_2^+ \rightarrow 2_1^+) = 3.69(58)$  W.u.] that we discuss below. The decay pattern of the  $0_3^+$  state at 1877.3 keV does not reflect the behavior of the expected  $0_\xi^+$  state at first glance. The measured  $B(E2; 0_3^+ \rightarrow 2_1^+) = 10.4(23)$  W.u. =  $0.24(6) \times B(E2; 2_1^+ \rightarrow 0_1^+)$  is about two times smaller than the  $B(E2; 0_3^+ \rightarrow 2_2^+) = 22.2(46)$  W.u. =  $0.52(13) \times B(E2; 2_1^+ \rightarrow 0_1^+)$ . The latter does not appear to be suppressed at all. This fact is in conflict with the O(5) selection rules. It indicates breaking of O(5) symmetry in  $^{128}\text{Xe}$ . Such symmetry breaking allows for the close-lying  $0_\xi^+$  ( $\tau = 0$ ) and  $0_\tau^+$  ( $\tau = 3$ ) configurations to mix with each other. Their mixing was already observed in Ref. [7] and must be taken into account for a quantitative clarification of the situation in  $^{128}\text{Xe}$ . The new data on absolute  $B(E2)$  values enable us to do this in an unambiguous way.

We consider the following admixed wave functions

$$|0_2^+\rangle = \alpha_\tau |0_\tau^+\rangle + \alpha_\xi |0_\xi^+\rangle, \quad (1)$$

$$|0_3^+\rangle = -\alpha_\xi |0_\tau^+\rangle + \alpha_\tau |0_\xi^+\rangle. \quad (2)$$

The  $0_\tau^+$  and  $0_\xi^+$  are orthonormal states. Since  $\langle 2_2^+ | T(E2) | 0_\xi^+ \rangle = 0$  and  $\langle 2_1^+ | T(E2) | 0_\tau^+ \rangle = 0$  we obtain

$$B(E2; 0_2^+ \rightarrow 2_1^+) = \alpha_\xi^2 B(E2; 0_\xi^+ \rightarrow 2_1^+), \quad (3)$$

$$B(E2; 0_3^+ \rightarrow 2_1^+) = \alpha_\tau^2 B(E2; 0_\tau^+ \rightarrow 2_1^+), \quad (4)$$

$$B(E2; 0_2^+ \rightarrow 2_2^+) = \alpha_\tau^2 B(E2; 0_\tau^+ \rightarrow 2_2^+), \quad (5)$$

$$B(E2; 0_3^+ \rightarrow 2_2^+) = \alpha_\xi^2 B(E2; 0_\xi^+ \rightarrow 2_2^+). \quad (6)$$

The mixing parameters can independently be determined from the appropriate ratios of experimental  $B(E2)$  values. We obtain  $\alpha_\xi^2/\alpha_\tau^2 = 0.35(10)$  from Eqs. (3) and (4) and  $\alpha_\xi^2/\alpha_\tau^2 = 0.42(11)$  from Eqs. (5) and (6). The agreement within uncertainties of these values obtained from independent observables confirms the consistency of the two-state mixing scenario. We proceed in using the average value  $\alpha_\xi^2/\alpha_\tau^2 = 0.39(7)$ , which results in  $\alpha_\tau^2 = 0.72(4)$  and  $\alpha_\xi^2 = 0.28(2)$ . Using these values in Eqs. (3) through (6), our data from Table I yield the E2 transition rates  $B(E2; 0_\tau^+ \rightarrow 2_2^+) = 76(10)$  and  $B(E2; 0_\xi^+ \rightarrow 2_1^+) = 14(2)$  W.u. for the unperturbed configurations.

From the mixing parameters and the energies of the perturbed levels, we determined the unperturbed energies of the pure configurations, which are  $E(0_\tau^+) = 1666$  and  $E(0_\xi^+) = 1795$  keV. We denote this unperturbed situation as  $^{128}\text{Xe}^*$  (cf. Fig. 3). We stress that the  $0_\xi^+$  configuration lies above the three-phonon one  $0_\tau^+$  configuration. This ordering is in qualitative contrast to the prediction made by the E(5) model [1].

As previously inferred from the  $R_{4/2}$  ratio,  $^{128}\text{Xe}$  lies in the E(5)-O(6) region, well-described by the O(5)-CBS model. Therefore, we compare the unperturbed experimental situation

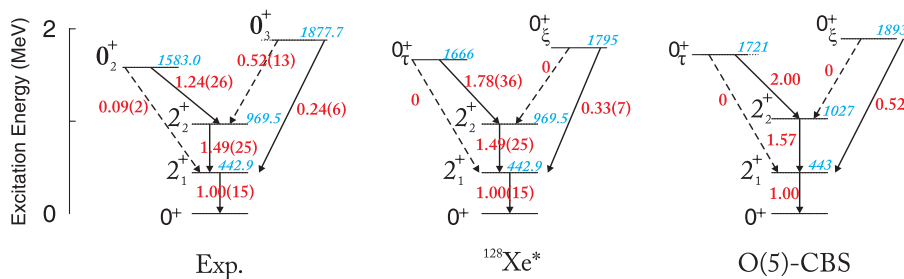


FIG. 3. (Color online) Energy-level scheme and  $B(E2)$  from  $0_2^+$  and  $0_3^+$  states of  $^{128}\text{Xe}$  (left), for the experimental unperturbed O(5)-symmetric states  $0_\tau^+$  and  $0_\xi^+$  ( $^{128}\text{Xe}^*$ , middle, see text), and for the O(5)-CBS model (right) from Ref. [7].

( $^{128}\text{Xe}^*$ ) to the prediction of the O(5)-CBS rotor model. The model's sole parameter  $r_\beta$  was fixed before [7] to reproduce the experimental  $R_{4/2}$  ratio of  $^{128}\text{Xe}$ . The agreement between  $^{128}\text{Xe}^*$  and the model predictions on the energies and  $E2$  transition rates is satisfactory as shown in Fig. 3. This includes the crucial ordering of the excited  $0_\tau^+$  and  $0_\xi^+$  configurations.

Our data and our analysis emphasizes the significance of the ordering of the excited  $0_\tau^+$  and  $0_\xi^+$  configurations for assigning the structure of a nucleus near the E(5) critical point. Therefore, it is interesting to examine the behavior of the observable  $\Delta_{0^+} = [E(0_\xi^+) - E(0_\tau^+)]/E(2_1^+)$ . It takes the values  $-1$  (harmonic vibrator),  $-0.56$  [E(5)], and  $0$  at the crossing point of the  $0_{\tau,\xi}^+$  configurations and becomes positive toward the O(6) limit. Along the chain of Xe isotopes we consider the experimental energies of the first and the second excited  $0^+$  states with dominant  $0_\tau^+$  or  $0_\xi^+$  assignment. The assignments of their dominant character were done for  $^{124}\text{Xe}$  ([22,23]),  $^{126}\text{Xe}$  ([24]),  $^{128}\text{Xe}$  ([7]), and  $^{130}\text{Xe}$  ([7]) already in the literature. These data are plotted in Fig. 4. The  $R_{4/2}$  ratios (top) decrease monotonically as a function of the neutron number from 2.48 for  $^{124}\text{Xe}$  to 2.04 for  $^{134}\text{Xe}$ . The value of 2.20 expected for E(5) is crossed between  $^{130}\text{Xe}$  and  $^{132}\text{Xe}$ . The  $0^+$  configurations cross between  $^{128}\text{Xe}$  and  $^{130}\text{Xe}$  (the middle of Fig. 4). The  $\Delta_{0^+}$  value for  $^{128}\text{Xe}$  is positive. This rules out  $^{128}\text{Xe}$  as a candidate for a realization of E(5) symmetry. We observe, however, that  $\Delta_{0^+} = -0.42$  for  $^{130}\text{Xe}$  making that nucleus a promising candidate for a close match of E(5) predictions.

Low-lying excited states of  $^{128}\text{Xe}$  were investigated by using the powerful Coulomb excitation method in inverse kinematics at Argonne National Laboratory. Nineteen absolute  $E2$  transition strengths were measured including the hitherto unknown  $B(E2)$  values from the  $0_2^+$  and  $0_3^+$  states. This enables us to unambiguously identify the main components of the  $0_\tau^+$  and  $0_\xi^+$  configurations. The ordering of these  $0^+$  configurations in  $^{128}\text{Xe}$  is opposite the prediction based on E(5) symmetry. Therefore, we conclude that  $^{128}\text{Xe}$  is not a close realization of E(5) symmetry, leaving  $^{130}\text{Xe}$  as the most likely candidate among the Xe isotopes. Our analysis highlights the importance of the relative energies of the first *two* excited  $0^+$  states and their  $E2$  decay rates as a robust test of E(5) symmetry. Similar

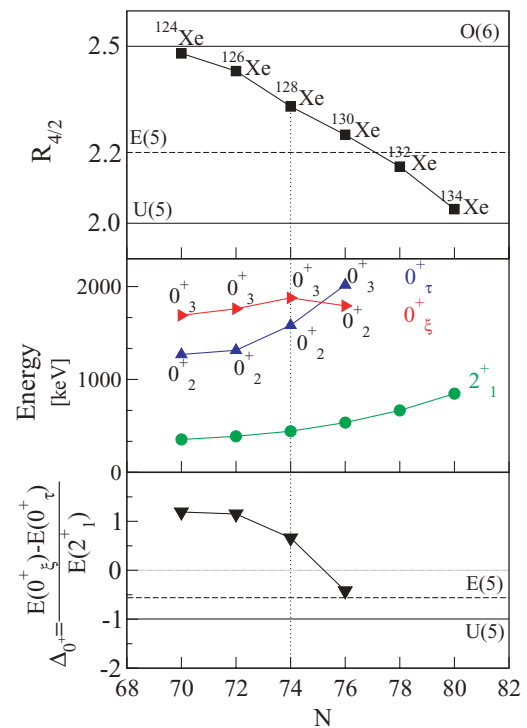


FIG. 4. (Color online) Evolution of  $R_{4/2} = E(4_1^+)/E(2_1^+)$  (top), energies of  $0_\tau^+$ ,  $0_\xi^+$ ,  $2_1^+$  states (middle), and  $\Delta_{0^+} = [E(0_\xi^+) - E(0_\tau^+)]/E(2_1^+)$  (bottom) for  $^{124,126,128,130,132,134}\text{Xe}$ .

tests on  $^{130}\text{Xe}$  and  $^{134}\text{Ba}$  will conclusively demonstrate how well E(5) is realized in these “best cases.”

We would like to thank the staff at ANL for their support during the experiments and A. Poves, F. Iachello, J. Jolie, A. Dewald, and P. von Brentano for discussions. This work was partially supported by the US Department of Energy, Office of Nuclear Physics, under Contract No. DE-AC02-06CH11357, by the DFG under Grant Nos. Pi 393/2-1 and SFB 634, by the German-Bulgarian exchange program under Grant Nos. D/08/02055 and DO02-25, and by the Helmholtz International Center for FAIR. G.R. acknowledges support from the Bulgarian NSF under contract DO 02-219.

- [1] F. Iachello, Phys. Rev. Lett. **85**, 3580 (2000).
- [2] F. Iachello, Phys. Rev. Lett. **87**, 052502 (2001).
- [3] F. Iachello, Phys. Rev. Lett. **91**, 132502 (2003).
- [4] R. F. Casten and N. V. Zamfir, Phys. Rev. Lett. **85**, 3584 (2000).
- [5] R. M. Clark *et al.*, Phys. Rev. C **69**, 064322 (2004).
- [6] R. F. Casten and P. Von Brentano, Phys. Lett. **B152**, 22 (1985).
- [7] D. Bonatsos, D. Lenis, N. Pietralla, and P. A. Terziev, Phys. Rev. C **74**, 044306 (2006).
- [8] N. Pietralla and O. M. Gorbachenko, Phys. Rev. C **70**, 011304(R) (2004).
- [9] I. Lee, Nucl. Phys. **A520**, c641 (1990).
- [10] P. J. Nolan, F. A. Beck, and D. B. Fossan, Annu. Rev. Nucl. Part. Sci. **45**, 561 (1994).
- [11] E. W. Schneider, M. D. Glascock, W. B. Walters, and R. A. Meyer, Phys. Rev. C **19**, 1025 (1979).
- [12] L. Goettig *et al.*, Nucl. Phys. **A357**, 109 (1981).
- [13] J. Srebrny *et al.*, Nucl. Phys. **A557**, 663c (1993).
- [14] U. Neumeyer *et al.*, Nucl. Phys. **A607**, 299 (1996).
- [15] I. Wiedenhöver *et al.*, Phys. Rev. C **56**, R2354 (1997).
- [16] P. F. Mantica Jr., B. E. Zimmerman, W. B. Walters, J. Rikovska, and N. J. Stone, Phys. Rev. C **45**, 1586 (1992).
- [17] M. Kanbe, K. Kitao, Nucl. Data Sheets **94**, 227 (2001).
- [18] K. Alder *et al.*, Rev. Mod. Phys. **28**, 432 (1956).
- [19] W. F. Mueller *et al.*, Phys. Rev. C **73**, 014316 (2006).
- [20] C. Y. Wu *et al.*, Nucl. Phys. **A607**, 178 (1996).
- [21] D. R. Bès, Nucl. Phys. **10**, 373 (1959).
- [22] V. Werner *et al.*, Nucl. Phys. **A692**, 451 (2001).
- [23] G. Rainovski *et al.*, Phys. Lett. **B683**, 11 (2010).
- [24] A. Gade *et al.*, Nucl. Phys. **A665**, 268 (2000).